Absolute parameters of the eclipsing binary V821 Cas from UBVRI light curves and radial velocities.[*] [†]

Ö. Çakırlı[1][‡], C. İbanoğlu[1], S. Bilir[2], E. Sipahi[1]

[1] *Ege University, Science Faculty, Department of Astronomy and Space Sciences, 35100 Bornova, İzmir, Turkey*
[2] *İstanbul University, Science Faculty, Department of Astronomy and Space Sciences, 34119 University, İstanbul, Turkey*

ABSTRACT

We present UBVRI photometric measurements and spectroscopic observations of the double-lined eclipsing binary V821 Cas. The radial velocities were obtained by means of the cross-correlation technique. Simultaneous analyses of the multi-band light curves and RVs give the absolute parameters for the stars as: M_1=2.05±0.07 $M_\odot$, M_2=1.63±0.06 $M_\odot$, R_1=2.31±0.03 $R_\odot$, R_2=1.39±0.02 $R_\odot$, T_{eff_1}=9 400±400 K, and T_{eff_2}=8 600±400 K. Analysis of the O–C residuals yielded an apsidal motion in the binary at a rate of $\dot\omega$=0°.0149±0°.0023 cycle^{-1}, corresponding to an apsidal period of U=118±19 yr. Subtracting the relativistic contribution we find that log k_{2obs}=-2.590 which is in agreement with the value predicted by theoretical models. Comparison with current stellar evolution models gives an age of 5.6×10^8 yr for the system.

Key words: binaries: stars: close - binaries: eclipsing-binaries: general - binaries: spectroscopic - stars: individual: V821 Cas

1 INTRODUCTION

V821 Cas (BD +52° 3571, Tycho 4001-1445-1, V=8^m.31, (B-V)=0.11) was discovered to be an eclipsing binary of early A spectral type, with a variability period of ∼1.8 days by the Hipparcos satellite (ESA, 1997). Değirmenci et al. (2003, 2007) determined an improved light curve and listed 25 photographic times of minima from which they derived an improved eclipse ephemeris. They obtained *BVR* light curves, and established that the orbit is eccentric from the displacement of the secondary minimum. Its components do not show intrinsic variability, they are well-separated, and well within their Roche lobes, which values them proper tests for stellar models.

Several times of minima for V821 Cas have appeared in the literature since, but no radial velocity measurements and multi-band light curves have been published. The aim of this work is to obtain the absolute parameters of the system. Along the next section we first present our spectroscopic data and the set of *UBVRI* light curves. Making use of the spectra we determine the parameters of the radial ve-

locity curve and perform a reliable estimation of the spectral types for both components. Then, using the results from the spectroscopy together with the our photometric data we analyze the light curves to obtain reliable solutions that allow to determine the rest of the parameters of the system.

2 OBSERVATIONS

2.1 Photometric observations

We report here new photometry of V821 Cas in the Bessell *UBVRI* bands. The photometric accuracy and the phase coverage (over 350 observations) are sufficient to guarantee a reliable determination of the light curve parameters thus permitting a critical evaluation of stellar models. The observations were carried out with the 0.40-m telescope located on Mt. Bakırlıtepe in September of 2007 at the TÜBİTAK National Observatory (TUG, located in south of Turkey). The telescope is equipped with a Apogee 1k×1k CCD (binned 2×2) and standard Bessel *UBVRI* filters.

The instrument with attached camera provide a field-of-view of 11′.3×11′.3. By placing V821 Cas very close to center of the CCD to get highest accuracy, we managed to strategically locate the binary on the chip together with two other stars of similar apparent magnitude. As comparison star we selected BD +52° 3575. The check star chosen to be BD +52° 3580. Both stars passed respective tests for intrin-

sic photometric variability and proved to be stable during time span of our observations.

We collected a total of 1600 points in the UBVRI bands. The resulting V-band magnitude differences (var-comp) are listed in Table 1 (available in electronic form at the CDS). A typical precision of the differential magnitudes is about 0.008 mag per measurement. Standard IRAF[1] tasks were used to remove the electronic bias and to perform the flat-fielding corrections. The IRAF task IMALIGN was used to remove the differences in the pixel locations of the stellar images and to place all the CCD images on the same relative coordinate systems. The data were analyzed using another IRAF task PHOT with no differential extinction effects taken into account given the relative small separation between the target and the comparison and check stars. The phase-folded light curves for the whole observations are shown in Fig. 5 with all bands.
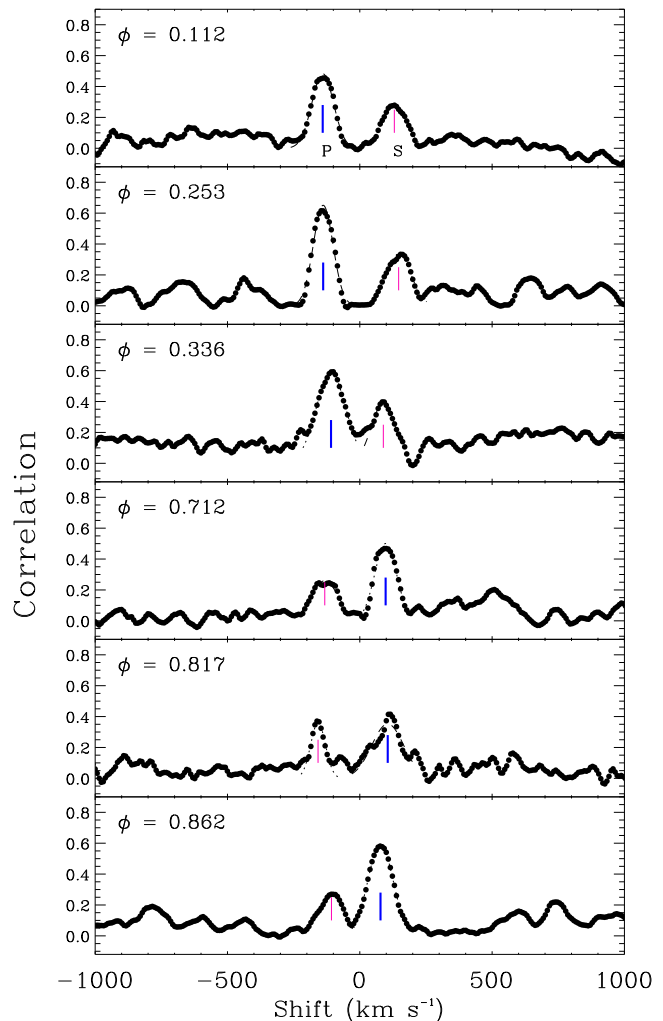
2.2 Spectroscopic observations

Spectroscopic observations have been performed with the échelle spectrograph (FRESCO) at the 91-cm telescope of Catania Astrophysical Observatory. The spectrograph is fed by the telescope through an optical fibre ($UV–NIR$, 100 μm core diameter) and is located, in a stable position, in the room below the dome level. Spectra were recorded on a CCD camera equipped with a thinned back–illuminated SITe CCD of 1k×1k pixels (size 24×24 μm). The cross-dispersed échelle configuration yields a resolution of about 20 000, as deduced from the full width at half maximum of the lines of the Th–Ar calibration lamp. The spectra cover the wavelength range from 4300 to 6650 Å, split into 19 orders. In this spectral region, and in particular in the blue portion of the spectrum, there are several lines useful for the measure of radial velocity, as well as for spectral classification of the stars.

The data reduction was performed by using the échelle task of IRAF package following the standard steps: background subtraction, division by a flat field spectrum given by a halogen lamp, wavelength calibration using the emission lines of a Th-Ar lamp, and normalization to the continuum through a polynomial fit.

Sixteen spectra of V821 Cas were collected during the 20 observing nights between August 2 and 23, 2006. Typical exposure times for the V821 Cas spectroscopic observations were between 2400 and 2600 s. The signal-to-noise ratio (S/N) achieved was between 70 and 115, depending on atmospheric condition. α Lyr (A0V), 59 Her (A3IV), ι Psc (F7V), HD 27962 (A2IV), and τ Her were observed during each run as radial velocity and/or rotational velocity templates. The average S/N at continuum in the spectral region of interest was 150–200 for the standard stars.
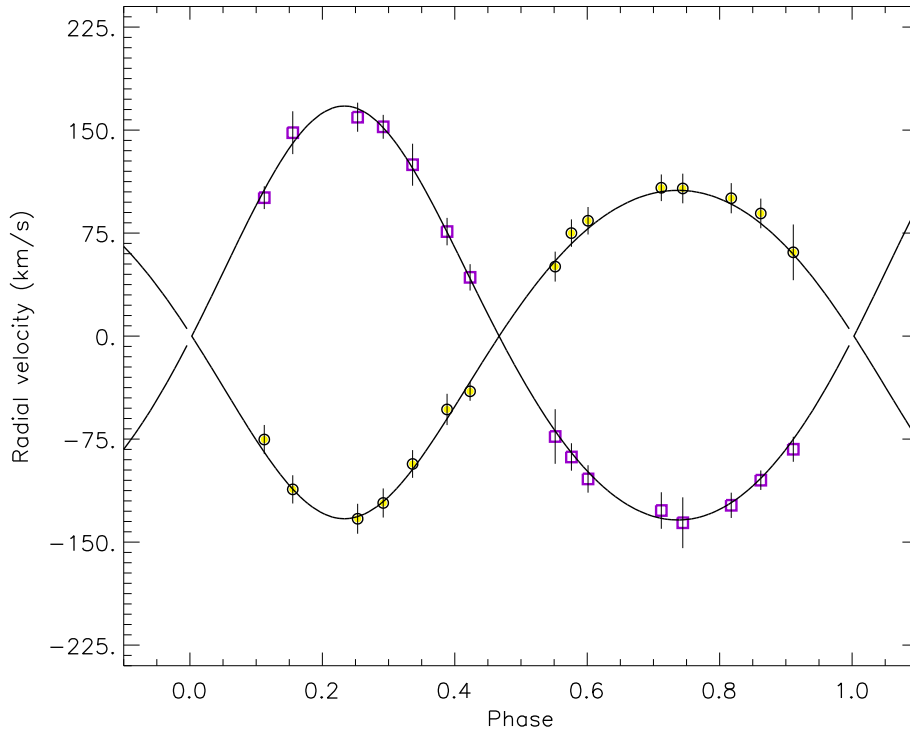

Figure 1. Sample of Cross Correlation Functions (CCFs) between V821 Cas and the radial velocity template spectrum (Vega) around the first and second quadrature.

3 SPECTROSCOPIC ANALYSIS

Double-lined spectroscopic binaries reveal two peaks, displacing back and forth, in the cross-correlation function (CCF) between variable and the radial velocity template spectrum as seen in Fig. 1. The location of the peaks allows to measure of the radial velocity of each component at the time of observation. The cross-correlation technique applied to digitized spectra is now one of the standard tools for the measurement of radial velocities in close binary systems.

The radial velocities of V821 Cas were obtained by cross–correlating of échelle orders of V821 Cas spectra with the spectra of the bright radial velocity standard stars α Lyr (A0V), 59 Her (A3IV) and ι Psc (F7V) (Nordström et al., 2004). For this purpose the IRAF task fxcor was used.

Fig. 1 shows examples of CCFs of V821 Cas near the first and second quadrature. The two non-blended peaks correspond to each component of V821 Cas. We applied the cross-correlation technique to five wavelength regions with well-defined absorption lines of the primary and secondary components. These regions include the following lines: Si III

---

[1] IRAF is distributed by the National Optical Observatory, which is operated by the Association of the Universities for Research in Astronomy, inc. (AURA) under cooperative agreement with the National Science Foundation

Figure 2. Radial velocity curve folded on a period of 1.7698 days, where phases 0,1,... are defined to be at mid–primary eclipse. The curves show the fit for an eccentric orbit, to the primary and secondary radial velocities. Points with error bars (error bars are masked by the symbol size in some cases) show the radial velocity measurements for the components of the system (primary: circles, secondary: squares).

4568 Å, Mg II 4481 Å, He I 5016 Å, He I 4917 Å, He I 5876 Å. The stronger CCF peak corresponds to the more massive component that also has a larger contribution to the observed spectrum. To better evaluate the centroids of the peaks (i.e. the radial velocity difference between the target and the template), we adopted two separate Gaussian fits for the case of significant peak separation.

The radial velocity measurements, listed in Table 2 together with their standard errors, are weighted means of the individual values deduced from each order (see, e.g., Frasca et al. 2006). The observational points and their error bars are displayed in Fig. 2 as a function of orbital phase as calculated by means of the ephemeris based on the photometric times of the primary eclipse described in Değirmenci et al. (2007).

The first detailed solution of both radial velocity curves of V821 Cas components is presented in this study. We found the semi-amplitude of the more massive, more luminous component to be $K_1=120\pm2$ km s^{-1} and $K_2=150\pm2$ km s^{-1} for the secondary component.

3.1   Spectral classification

We have used our spectra to classify the primary component of V821 Cas. For this purpose we have degraded the spectral resolution from 20 000 to 3 000, by convolving them with a Gaussian kernel of the appropriate width, and we have measured the equivalent width (EW) of photospheric absorption lines useful for the spectral classification. We have followed the procedures of Hernández et al. (2004), choosing hydrogen and helium lines in the blue-wavelength region, where the contribution of the secondary component to the observed spectrum is negligible. From several spectra we measured $EW_{H\gamma} = 11.3 \pm 0.9$ Å, $EW_{H\alpha} = 9.89 \pm 0.11$ Å, $EW_{H\beta} = 10.79 \pm 0.13$ Å, and $EW_{MgII\lambda4481} = 0.31 \pm 0.04$ Å.

From the calibration relations EW–Spectral-Type of Hernández et al. (2004), we have derived a spectral type A1V with an uncertainty of about 1.0 spectral subclass. The effective temperature deduced from the calibrations of Drilling & Landolt (2000) or de Jager & Nieuwenhuijzen (1987) is about 9 400 K (A1V). The spectral-type uncertainty leads to a temperature error of $\Delta T_{\rm eff} \approx 400$ K.

3.2   Reddening

The measurement of reddening is a key step in determining the absolute temperature scale (and therefore the distance) of eclipsing binaries. In addition to moderate distance determined by the Hipparcos mission, some reddening is expected for V821 Cas due to its low galactic latitude (l=115°.10, $b = -8^{\circ}.40$).

Our spectra cover the interstellar Na I (5890 and 5896 Å) doublets, which is excellent estimators of the reddening as demonstrated by Munari & Zwitter (1997). They calibrated
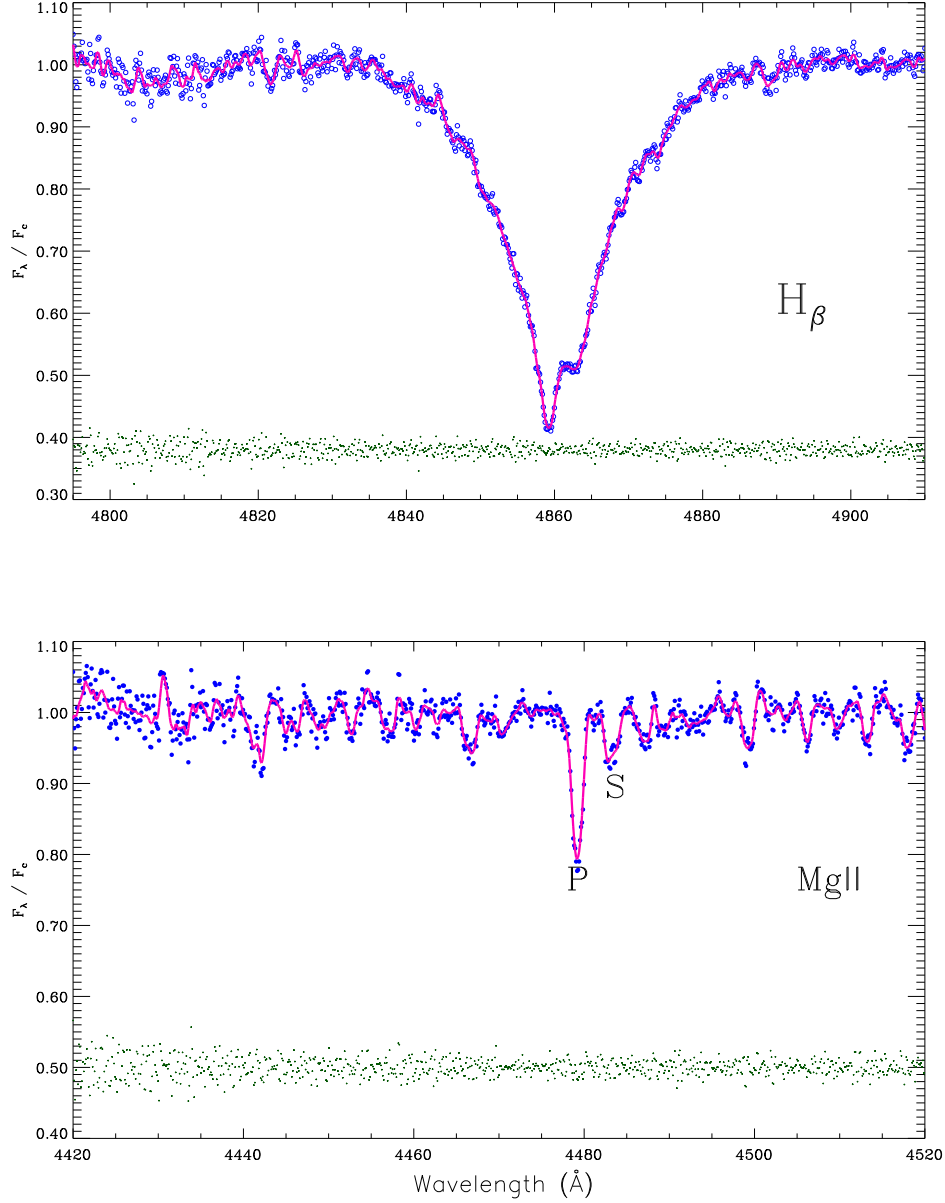
Figure 3. Observed spectrum of V821 Cas (large dots) in the $\lambda4861$ H$_\beta$ region (upper panel) and Mg II $\lambda4481$ (bottom). The synthetic spectrum (A1V+A4V) is displayed with continuous line in the same boxes. The differences (observed-synthetic, shifted) are plotted in the bottom of each panel.

a tight relation linking the Na I D2 (5890 Å) and K I (7699 Å) equivalent widths with the E(B-V) reddening. On spectra obtained at quadratures, lines from both components are un-blended with the interstellar ones, which can therefore be accurately measured. We derive an equivalent width of 0.34 ± 0.02 Å for only NaI, which corresponds to E(B-V)= 0.147 ± 0.011 mag. K I interstellar line is out of our spectral range as given in wavelength region in previous section.

3.3   Rotational velocity

The width of the cross-correlation profile is a good tool for the measurement of $v \sin i$ (see, e.g., Queloz et al. 1998). The rotational velocities ($v \sin i$) of the two components were obtained by measuring the FWHM of the CCF peaks in nine high-S/N spectra of V821 Cas acquired close to the quadratures, where the spectral lines have the largest Doppler-

Table 2. Radial velocities of the V821 Cas' components. The columns give the heliocentric Julian date, the orbital phase (according to the ephemeris given by Değirmenci et al. 2006), the radial velocities of the two components with the corresponding errors, and the average S/N of the spectrum.

HJD 2 453 000+	Phase	Star 1 $\mathbf{V}_p$	σ	Star 2 $\mathbf{V}_s$	σ	$<S/N>$
53953.6017	0.3363	-93.1	6.1	124.8	9.3	88[a]
53955.6040	0.4677	-3.3	3.2	—	—	76
53957.5655	0.5761	75.0	6.4	-88.0	8.8	80
53958.5906	0.1553	-111.6	8.3	148.1	11.6	97[a]
53970.5469	0.9112	61.0	6.3	-82.4	12.1	75
53973.5377	0.6012	84.0	4.8	-104.0	8.1	95[a]
53975.5607	0.7443	107.5	4.8	-135.9	8.5	106[a]
53980.5290	0.5516	50.6	4.9	-73.1	9.9	90
53981.5213	0.1123	-75.3	3.6	100.8	7.1	90[a]
53982.5825	0.7119	108.0	2.7	-127.0	7.3	110[a]
53983.5405	0.2533	-133.0	2.9	159.4	6.6	113[a]
53983.6089	0.2919	-121.5	2.6	152.4	3.7	95
53984.5390	0.8175	100.4	3.0	-123.2	5.2	97
53984.6180	0.8621	89.3	1.8	-104.9	7.1	101[a]
53985.5492	0.3883	-53.4	3.4	76.1	6.0	100[a]
53985.6109	0.4231	-40.2	3.9	42.8	5.6	72

[a] Used also for rotational velocities ($v \sin i$) measurements.

shifts. In order to construct a calibration curve FWHM–$v \sin i$, we have used an average spectrum of HD 27962, acquired with the same instrumentation. Since the rotational velocity of HD 27962 is very low but not zero ($v \sin i \simeq 11$ km s^{-1}, e.g., Royer, Zorec & Fremat 2004 and references therein), it could be considered as a useful template for A-type stars rotating faster than $v \sin i \simeq 10$ km s^{-1}. The spectrum of HD 27962 was synthetically broadened by convolution with rotational profiles of increasing $v \sin i$ in steps of 5 km s^{-1} and the cross-correlation with the original one was performed at each step. The FWHM of the CCF peak was measured and the FWHM-$v \sin i$ calibration was established. The $v \sin i$ values of the two components of V821 Cas were derived from the FWHM of their CCF peak and the aforementioned calibration relations, for a few wavelength regions and for the best spectra. This gave values of 70±1 km s^{-1} for the primary star and 57±1 km s^{-1} for the secondary star.

We classified the spectral type of the primary component as an A1 type main-sequence star. The secondary component appears to be an A4V star (see § 5). The spectral types of the standard stars α Lyr and 59 Her are very close to the primary and secondary component of the V821 Cas, respectively. For the construction of the synthetic spectrum of the system the spectra of the standard stars, obtained with the same instrumentation, have been rotationally broadened by convolution with the appropriate rotational profile and then co-added, properly weighted by using physical parameters (T_1, T_2, R_1, R_2, $vsini_{12}$) of the components as input parameters and, then, Doppler-shifted according to the radial velocities of the components. In Fig. 3 we show the simulation of the spectrum of V821 Cas with the standard stars.

Table 4. Apsidal motion parameters for V821 Cas.

Anomalistic Period P_a	1.769813±0.000040
Reference minimum time T_0 HJD	51 767.3481±0.0008
Periastron longitude at T_0,$\omega°$	148±4
Apsidal motion rate $\dot{\omega}$ cycle^{-1}	0.0149±0.0023
Orbital eccentricity e	0.138±0.011
Apsidal motion rate U yr	117±19

4 EPHEMERIS AND APSIDAL MOTION

V821 Cas has a moderate eccentric orbit. All available times of minimum light covering about 3100 orbital cycles were collected by Değirmenci et al. (2007). Their analysis of the O-C residuals yields for the first time a period of apsidal motion to be 158 yr.

All available times of minimum light were collected from literature are listed in Table 4 together with the new timings obtained in this study. The O-C residuals indicate the differences between the observed and calculated times obtained with linear ephemeris,

$$MinI(HJD) = 2\,451\,767.3504 + 1^d.7697397 \times E \qquad (1)$$

The method of Gimenez & Garcia-Pelayo (1983) was adopted to carry out the apsidal motion parameters with the use of differential-correction approximations. The method is successively relates the derived apsidal motion parameters to the observed times of minima. We used some subroutines in the analysis of the O-C values, supplied by Ö. L. Değirmenci. Two secondary and one primary eclipse timings given by Otero (2005) were omitted from the analysis due to the large deviations from the others. These timings were estimated from very few observations, either in ascending or descending branch of the eclipses. Assuming the orbital inclination $i \sim 83°$ from the light curve analysis (see next section) and using the residuals in Table 4 we obtained the parameters of apsidal motion with a weighted least-square solution.

The apsidal motion resulting from the fit is $\dot{\omega}$=0°.0149 ±0°.0023 cycle^{-1}, which is significant at the 6.5σ level. The sidereal and anomalistic periods (P_s and P_a), as well as the apsidal motion period $U = 118±19$ yr are listed in Table 4. A plot of the O-C deviations of the times of minimum from the linear terms of the apsidal motion is shown in Fig. 4 along with the predicted deviations. In the bottom panel of Fig. 4 we show the differences between observed and computed timings, taking into account apsidal motion. The apsidal motion parameters given in Table 4 are only preliminary results because the data we used cover only 14 % of the apsidal motion period.

5 SIMULTANEOUS LIGHT CURVES AND RADIAL VELOCITIES ANALYSES

In order to obtain the values of the main physical parameters of the binary components and to determine the orbital inclination (i) of the system (necessary to deduce stellar masses from the $M_{1,2} \sin^3 i$ derived from the RV curves) we applied a numerical eclipsing binary model to the *UBVRI* observations. We choose the Wilson–Devinney (W–D) code imple-
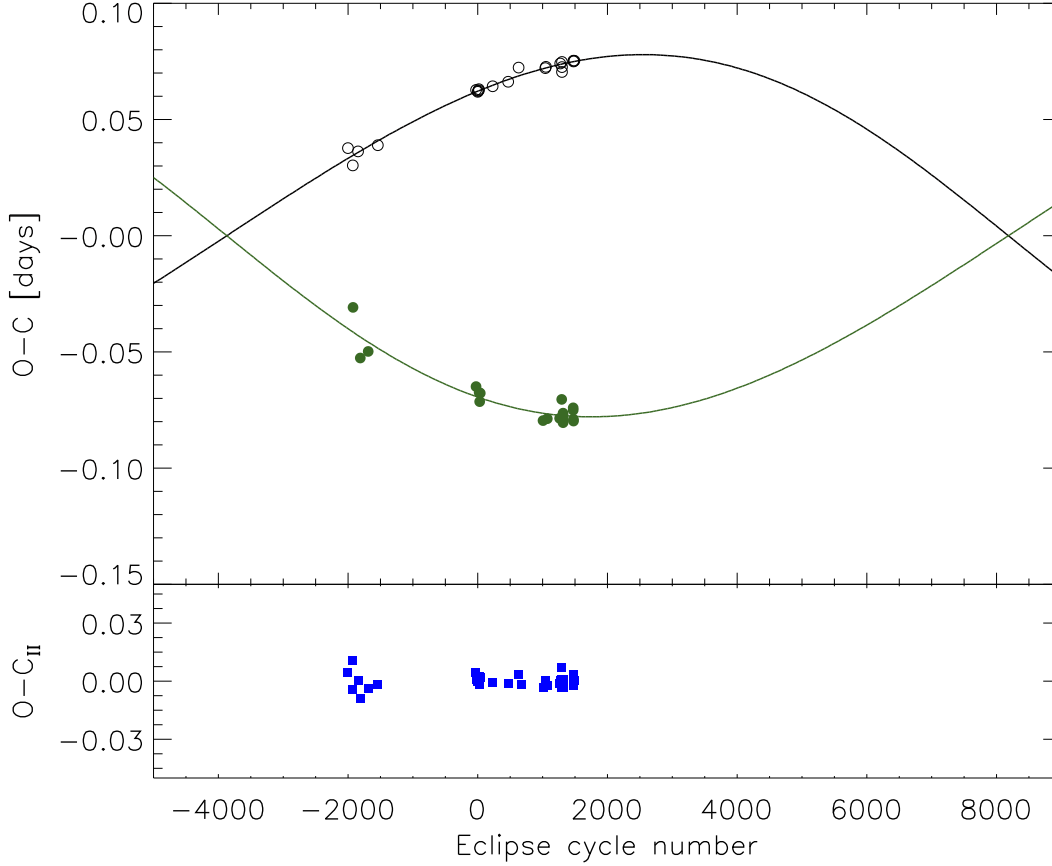
Figure 4. Representation of the best-fitting apsidal motion parameters. The upper panel shows the observed times of primary (open circles) and secondary (filled circles) minima, continuous line are best-fitting curves of primary and secondary minima. The lower panel shows the residual of the O-C values from the fitted curves.

mented into the PHOEBE package tool by Prsa & Zwitter (2005) for the LC and differential correction (DC) fits.

The code was set in Mode–2 for detached binaries with no constraints on the potentials. The effective temperature (T_1) of the primary star was fixed at 9400±400 K defined in §3. The simplest considerations were applied for the parameters of the stars in the model, that is, stars were considered as black bodies, approximate reflection model (MREF=1) was adopted, and no third light or spots were included. Gravity–darkening exponents $g_1 = g_2 = 1$ and bolometric albedos $Alb_1 = Alb_2 = 1$ were set for radiative envelopes. We used square root limb–darkening law. Bolometric limb-darkening coefficients were taken from Van Hamme (1993).

The mass ratio, $q=M_2/M_1$, is very important parameter in the light curve analysis, because the WD code is based on Roche geometry which is sensitive to this quantity. The mass ratio of 0.795 determined from the radial velocities was kept as a fix value. The iterations were carried out automatically until convergence and a solution was defined as the set of parameters for which the differential corrections were smaller than the probable errors. The light curves were analyzed individually and the weighted means of the parameters i, T_2, Ω_1, Ω_2, r_1 and r_2 were computed. Our final results are

listed in Table 5 and the computed light curves are shown as continuous lines in Fig. 5. The uncertainties assigned to the adjusted parameters are the internal errors provided directly by the Wilson-Devinney code. In the bottom panel of Fig.5 the residuals between observed and computed fluxes are also plotted. The residuals reveal that the binary model may represent the observed light curves successfully.

6   DISCUSSION AND CONCLUSIONS

6.1   Absolute dimensions and distance to the system

Combination of the parameters obtained from light curves and RVs yield the absolute dimensions of the system, which are presented in Table 6. The standard deviations of the parameters have been determined by JKTABSDIM[2] code, which calculates distance and other physical parameters using several different sources for bolometric corrections (Southworth et al. 2005). The radii of the components were

---

[2] This can be obtained from http://www.astro.keele.ac.uk/∼jkt/codes.html

Table 3. Times of minimum light of V821 Cas. The O-C values refer to the difference between the observed and calculated values.

Cycle number	Minimum time (HJD-240 0000)	O-C	Ref.	Cycle number	Minimum time (HJD-240 0000)	O-C	Ref.
-2002.0	48224.3680	0.0377	1	672.5	52957.4215	-0.0762	4
-1927.0	48357.0910	0.0303	1	1051.0	53627.4166	0.0727	4
-1923.5	48363.2240	-0.0308	1	1072.5	53665.3146	-0.0787	4
-1846.0	48500.4459	0.0363	2	1006.5	53548.5110	-0.0796	7
-1811.5	48561.4130	-0.0526	1	1042.0	53611.4884	0.0721	7
-1689.5	48777.3240	-0.0498	1	1262.5	54001.5652	-0.0786	7
-1541.0	49040.2190	0.0389	1	1272.0	54018.5304	0.0741	7
-197.5	51417.6940**	-0.1306	1	1294.5	54058.2050	-0.0704	8
-179.0	51450.6030**	0.0382	1	1299.0	54066.3097	0.0704	8
-162.5	51479.6370**	-0.1285	1	1299.0	54066.3118	0.0725	8
-26.5	51720.3851	-0.0649	3	1299.0	54066.3140	0.0747	8
-26.0	51721.3976	0.0627	3	1315.5	54095.3595	-0.0804	8
0.0	51767.4100	0.0619	4	1315.5	54095.3601	-0.0798	8
4.0	51774.4893	0.0622	4	1315.5	54095.3610	-0.0789	8
17.0	51797.4962	0.0625	4	1315.5	54095.3625	-0.0774	8
17.0	51797.4967	0.0630	4	1315.5	54095.3636	-0.0763	8
21.5	51805.3300	-0.0675	4	1471.5	54371.4442	-0.0751	8
29.5	51819.4840	-0.0714	4	1471.5	54371.4452	-0.0741	8
38.5	51835.4153	-0.0678	4	1475.5	54378.5192	-0.0790	8
230.0	52174.4524	0.0643	4	1476.0	54379.5584	0.0753	8
469.0	52597.4220	0.0662	5	1476.5	54380.2882	-0.0798	8
630.0	52882.3561	0.0723	6	1477.0	54381.3278	0.0750	8
672.5	52957.4215	-0.0762	4	1490.0	54404.3347	0.0753	8

** Rejected from the fit owing to a large O-C value.

Ref: (1) Otero (2005), (2) ESA (1997),(3) Bulut & Demircan (2003), (4) Değirmenci et al. (2003, 2007), (5) Ak & Filiz (2003), (6) Bakış et al. (2003), (7) Brat et al. (2007), (8) This study.

Table 5. Results from the simultaneous solution of *UBVRI* band light curves of V821 Cas.

Parameter	Value
$i(°)$	82.6±0.1
$e(°)$	0.127±0.007
$\omega(°)$	155±4
T_1 (K)	9400[Fix]
T_2 (K)	8600±17
Ω_1	5.067±0.014
Ω_2	6.693±0.035
q_{spec}	0.795
$L_1/(L_{1+2})_U$	0.825±0.001
$L_1/(L_{1+2})_B$	0.794±0.003
$L_1/(L_{1+2})_V$	0.801±0.004
$L_1/(L_{1+2})_R$	0.790±0.004
$L_1/(L_{1+2})_I$	0.781±0.008
r_1	0.2434±0.0013
r_2	0.1466±0.0017
$\Delta\phi$	-0.0424±0.0005
χ^2	0.002

Table 6. Fundamental parameters of V821 Cas.

	V821 Cas	
Parameter	Primary	Secondary
Spectral Type	A1V±1	A4V±1
a (R$_\odot$)		9.496±0.099
V_γ (km s^{-1})		-0.05±0.01
i (°)		82.6±0.1
q		0.795±0.017
Mass (M$_\odot$)	2.046±0.067	1.626±0.058
Radius (R$_\odot$)	2.311±0.028	1.392±0.022
log g (cgs)	4.021±0.007	4.362±0.012
T_{eff} (K)	9400±400	8600±400
$(v\sin i)_{obs}$ (km s^{-1})	70±1	57±1
$(v\sin i)_{calc.}$ (km s^{-1})	66±1	40±1
log $(L/L_\odot)$	1.58±0.06	0.98±0.01
d (pc)		260±12
J, H, K_s (mag)*	7.978±0.018, 8.007±0.027, 7.956±0.027	
$\mu_\alpha cos\delta, \mu_\delta$(mas yr^{-1})**	-2.51±0.59, -5.95±0.62	
U, V, W (km s^{-1})	4.77±0.70, 1.07±0.34, -6.82±0.80	

*2MASS All-Sky Point Source Catalogue (Cutri et al. 2003)
**Newly Reduced Hipparcos Catalogue (van Leeuwen 2007)

estimated with uncertainties of 1.2 % and 1.6%. However, the uncertainties on the masses, being 3.3 % and 3.6 %, are slightly larger than the criteria of Andersen (1991) for the necessary precision of absolute dimensions of stars to be used for comparison with theoretical models.

An inspection of the temperatures, masses and radii of the component stars reveals a binary system composed of two main-sequence stars. The temperature T_{eff1} = 9400 K, mass M_1 = 2.04 M$_\odot$ and radius R_1 = 2.31 R$_\odot$ of the

primary are consistent with the spectral type of A1V, and the temperature T_{eff1} = 8450 K, mass M_2 = 1.62 M$_\odot$ and radius R_2 = 1.39 R$_\odot$ of the secondary are consistent with an A4V spectral type star.

The colour excess $E(B - V)$ for a star may also be determined from the wide-band photometry. For calculation
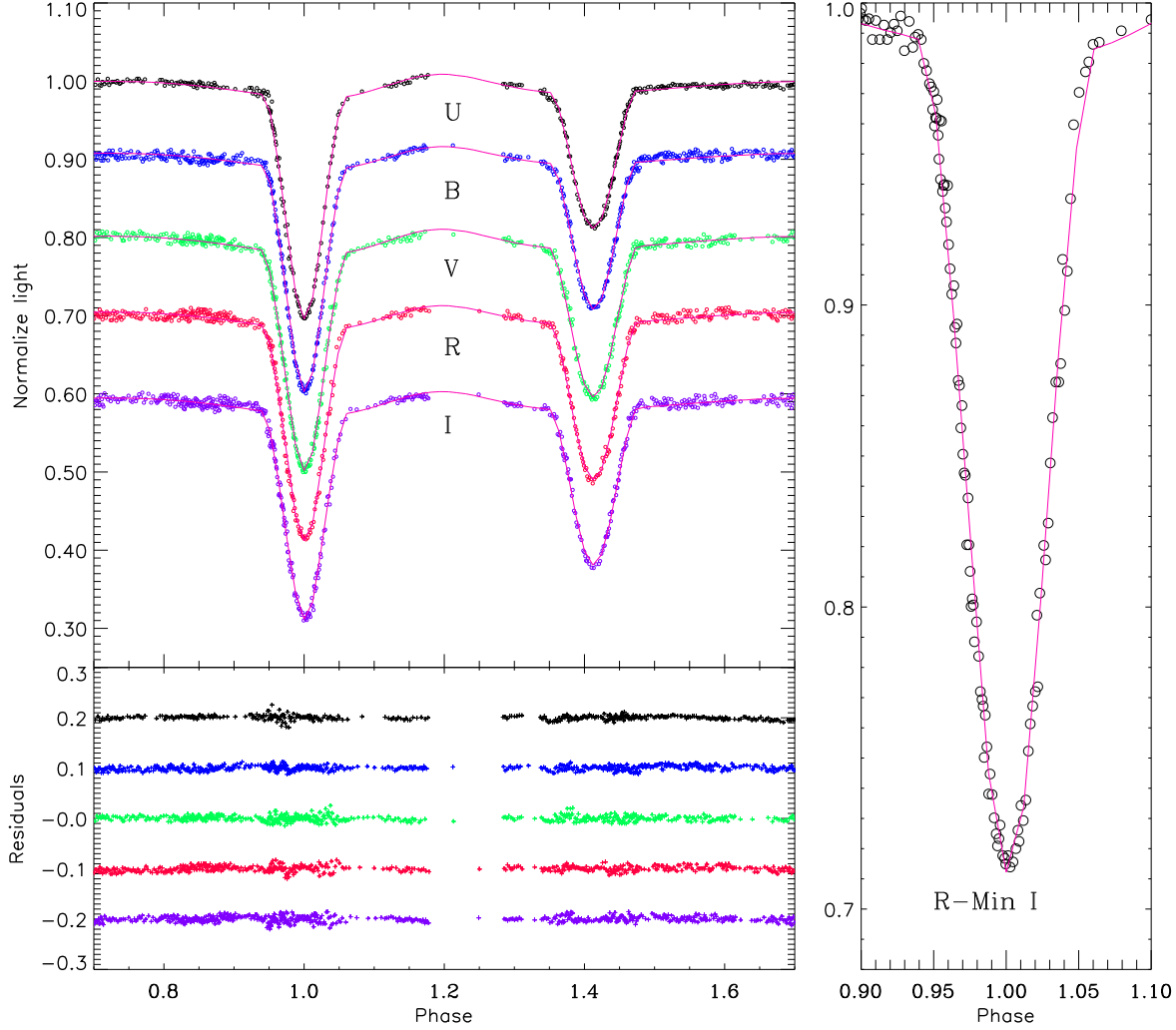
Figure 5. Observed phased light curves of V821 Cas with the best-fitting Phoebe model light curves. For clarity the *UBVRI* light curves and residuals of the fit (lower panel) have been offset by constant amounts as shown in figure. The right panel expands the region near the primary minimum for the R-band.

the reddening-free $Q - parameter$ we used the well-known equation below,

$$Q = (U - B) - [E(U - B)/E(B - V)] \times (B - V), \quad (2)$$

for stars from O9 to A2. The average ratio of colour excesses for stars from O8 to A2 was adopted as $[E(U - B)/E(B - V)] = 0.72 \pm 0.03$ (Hovhannessian 2004). The standard relation between Q_{UBV} and $(B - V)_0$ was also given in Hovhannessian's study. For calculation of the total absorption in the visual magnitude the following relation, the ratio of selective-to-total extinction in the V band,

$$[A_V/E(B - V)] = 3.30 + 0.28(B - V)_0 + 0.04E(B - V), (3)$$

given by Drilling & Landolt (2001) was adopted.

Using the observed visual magnitude and color indexes

given by Oja (1985) as V=8.26, U-B=0.07 and B-V=0.11 mag we compute the reddening-free parameter as $Q = -0.009$. Using the tables given by Hovhannessian (2004) we find the intrinsic colour index of $(B - V)_0 = -0.021$ mag and then the colour excess of $E(B - V) = 0.131 \pm 0.020$ mag for the system. The colours of the system were the average of three measurements. We should mention that there is no clue about the date of observations obtained, i.e. orbital phase. This value is in agreement with the E(B-V)=0.147 determined from the spectra given in §3.2.

Using the two $E(B - V)$ values derived from photometric and spectroscopic data we calculated the de–reddening distance modulus of the system. To estimate the bolometric magnitudes of the components we adopted M_{bol}=4.74 mag for the Sun. Using the bolometric corrections given by

Drilling & Landolt (2000) and Girardi et al. (2002) we estimate the distance to the system as 260 and 274 pc, respectively, with an uncertainty of 12 pc. However, the average distance to the system is estimated to be 206^{+42}_{-29} pc from the trigonometric parallax measured by the Hipparcos mission.

6.2 Internal structure

Our detection of the apsidal motion rate of the V821 Cas in §4 provides the opportunity to test the models of stellar internal structure. In addition to the classical Newtonian contribution, the observed rate of rotation of apsides includes also the contributions arising from General Relativity. The theory of General Relativity estimates the relativistic contribution to observed rate as the following Einstein formula:

$$\dot{\omega}_{rel} = 5.45 \times 10^{-4} \frac{1}{1-e^2} (\frac{M_1 + M_2}{P_a})^{2/3} \qquad (4)$$

where $M_i (i = 1, 2)$ denotes the individual masses of the components in solar mass, e is the orbital eccentricity (from radial velocity analysis) and P_a is the anomalistic period of the system in days. Use of equation (4) for V821 Cas yields the relativistic contribution of $0°.0009$ cycle^{-1} which is only 6 per cent of the observed rate. Removing the relativistic contribution from the observed rate of apsidal motion, one can calculate the observational average value of internal structure constant (k_{2obs}) using the following formula:

$$\bar{k}_{2obs} = \frac{1}{c_{21} + c_{22}} \frac{\dot{\omega}}{360}, \qquad (5)$$

where $c_{2i} (i = 1, 2)$ are the functions of the orbital eccentricity, fractional radii and masses of the components and ratio of the rotational velocities of the component stars to the Keplerian velocity. The observed average value of $\log k_2$ is found to be -2.56±0.07 from Eq. (5). The theoretical internal structure constants for the components ($\log k_{2theo1,2}$) are taken from the theoretical calculations of Claret (2004). Among the tabulated values, interpolation for the masses and $\log g$ of the component star V821 Cas yielded -2.48 and -2.37 for the primary and secondary components, respectively. The mean theoretical value of internal structure constant was computed as $\log k_{2theo}$=-2.43 which is in agreement with that of observed within 2σ level. The internal structure constant obtained from the O-C analysis is smaller by 35 % than predicted from the theory. The present analysis shows that the component stars are more concentrated in mass than predicted by theoretical calculations.

6.3 Evolutionary stage and age of the system

In Fig. 6, we plot the location of V821 Cas stellar components in $\log T_{eff} - \log g$ diagram. The evolutionary tracks for masses 1.6, 2.0 $M_\odot$ and $z = 0.008$ (Girardi et al. 2002) are also shown in this figure. Higher metallicity tracks given by Girardi et al. do not match with the observed properties of the components. An isochrone corresponding to an age of 5.6×10^8 yr, computed from Girardi et al. (2002)[3] is also shown in Fig. 6. The effective temperature of the primary

[3] We computed the isochrones using the facility available in the web site: http://stev.oapd.inaf.it/~lgirardi/cgi-bin/cmd

component appears to be slightly higher than the model for 2 $M_\odot$. However, when the uncertainties of the effective temperatures of the components are taken into account it is seen that the deviations from the models are less than 1σ level. The diagram suggests that both components of V821 Cas are main sequence stars, relatively young with an age of about 560 Myr.

6.4 Population type and kinematical analysis of V821 Cas

To study the kinematical properties of V821 Cas, we used the system's center-of-mass' velocity, distance and proper motion values, which are given in Table 6. The proper motion data were taken from newly reduced Hipparcos catalogue (van Leeuwen 2007), whereas the center-of-mass velocity and distance are obtained in this study. The system's space velocity was calculated using Johnson & Soderblom's (1987) algorithm. The U, V and W space velocity components and their errors were obtained and given in Table 6. To obtain the space velocity precisely the first-order galactic differential rotation correction was taken into account (Mihalas & Binney 1981), and -1.08 and 0.65 kms^{-1} differential corrections were applied to U and V space velocity components, respectively. The W velocity is not affected in this first-order approximation. As for the LSR correction, Mihalas & Binney's (1981) values (9, 12, 7)$_\odot$ kms^{-1} were used and the final space velocity of V821 Cas was obtained as $S = 19.36$ kms^{-1}. This value is in agreement with other young stars space velocities.

To determine the population type of V821 Cas the galactic orbit of the system was examined. Using Dinescu et al. (1999) N-body code, the system's apogalactic (R_{max}) and perigalactic (R_{min}) distances were obtained as 9.09 and 8.07 kpc, respectively. Also, the maximum possible vertical separation from the galactic plane is $|z_{max}|$=50 pc for the system. When determining the ellipticity the following formula was used:
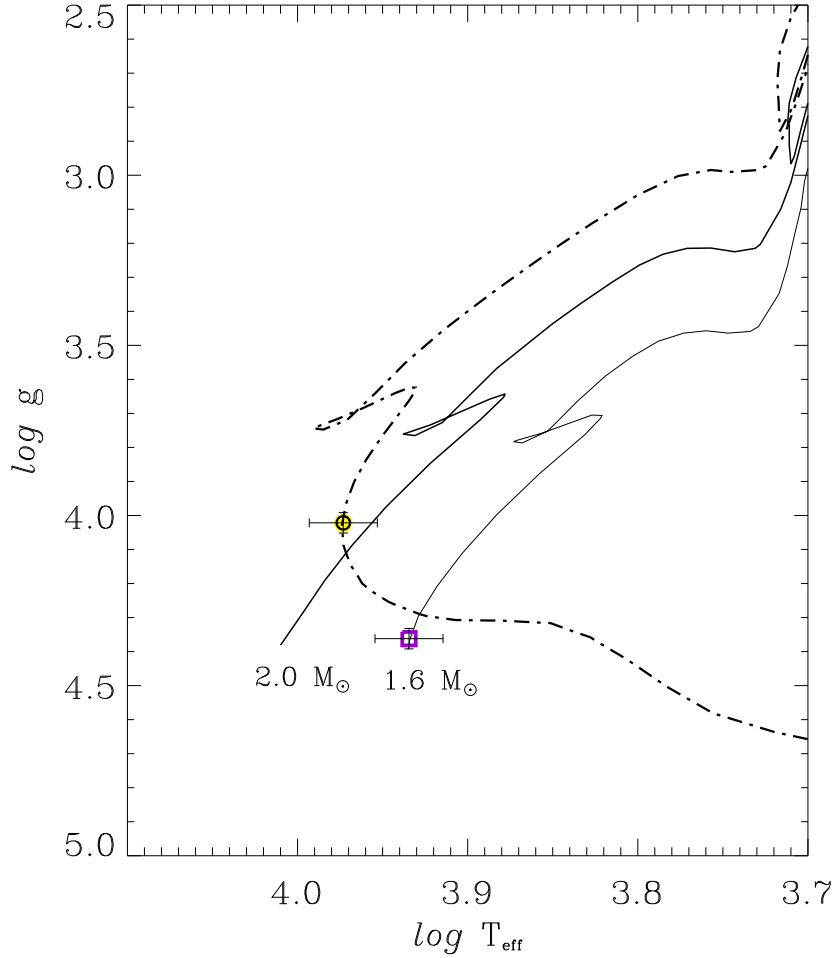
$$e = \frac{R_{max} - R_{min}}{R_{max} + R_{min}}. \qquad (6)$$

The ellipticity was calculated as $e = 0.059$. This value shows that V821 Cas is orbiting the Galaxy in an almost circular orbit and that the system belongs to the young thin-disc population.

Figure 6. Location of the two stellar components of V821 Cas in log T_{eff}- log g diagram, together with evolutionary models for the masses of 1.6 and 2.0 M$_\odot$ (Girardi et al. 2002) and the isochrones of an age $t=5.6\times10^8$ years (long-dashed-dotted line). The open circle corresponds to the primary and the open square to the secondary.

REFERENCES

Ak H., Filiz N., 2003, IBVS, 5462

Andersen J., 1991, A&ARv, 3, 91

Bakış V., Bakış H., Erdem A., Çiçek C., Demircan O., Budding E., 2003, IBVS, 5464

Bessell M. S., Castelli F., Plez B., 1998, A&A, 337, 321

Bilir S., Ak T., Soydugan E., Soydugan F., Yaz E., Ak F., Eker Z., Demircan O., Helvacı M., 2008, AN, 329, 835

Bulut İ., Demircan O., 2003, IBVS, 5476

Brat L., Zejda M., Svoboda P., 2007, B.R.N.O. Contributions #34

Claret A., 2004, A&A, 424, 919

Cutri R. M., et al., 2003, The IRSA 2MASS All-Sky Point Source Catalog, NASA/IPAC Infrared Science Archive. http://irsa.ipac.caltech.edu/applications/Gator/

de Jager C., Nieuwenhuijzen H., 1987, A&A, 177, 217

Değirmeci Ö. L., Bozkurt Z., Yakut K. et al., 2003, IBVS, 5386

Değirmeci Ö. L., Bozkurt Z., Yakut K. et al., 2007, NewA, 322, 326

Dinescu, D. I., Girardi, T. M., van Altena, W. F., 1999, AJ, 117, 1792

Drilling J. S., Landolt A. U., 2000, Allen's astrophysical quantities, 4th ed. Edited by Arthur N. Cox. ISBN: 0-

387-98746-0. Publisher: New York: AIP Press; Springer, 2000, p.381

ESA 1997, ESA SP-1200, The Hipparcos and Tycho Catalogues. ESA, Noordwijk

Frasca A., Guillout P., Marilli E., Freire Ferrero R., Biazzo K., Klutsch A., 2006, A&A, 454, 301

Gimenez A., Garcia-Pelayo J. M., 1983, Ap&SS, 92, 203

Girardi L., Bertelli G., Bressan A., Chiosi C., Groenewegen M. A. T., Marigo P., Salasnich B., Weiss A., 2002, A&A, 391, 195

Hernández J., Calvet N., Briceño C., Hartmann L., Berlind P., 2004, AJ, 127, 1682

Hovhannessian R. Kh., 2004, Ap, 47, 499

Johnson D. R. H., Soderblom D. R., 1987, AJ, 93, 864

Mihalas D., Binney J., 1981. in Galactic Astronomy, 2nd edition, Freeman, San Fransisco, p.181

Munari U., Zwitter T., 1997, A&A, 318, 269

Nordström B., Mayor M., Holmberg J., Pont F., Jorgensen B. R., Olsen E. H., Udry S., Mowlavi N., 2004, A&A, 418, 989

Oja T., 1985, Ap&SS, 59, 461

Otero S. A., 2005, IBVS, 5631

Prša A., Zwitter T., 2005, ApJ, 628, 426

Queloz D., Allain S., Mermilliod J.-C., Bouvier J., Mayor M., 1998, A&A, 335, 183

Royer F., Zorec J., Fremat Y., 2004, "The A-Star Puzzle", held in Poprad, Slovakia, July 8-13, 2004. Edited by J. Zverko, J. Ziznovsky, S.J. Adelman, and W.W. Weiss, IAU Symposium, No. 224. Cambridge, UK: Cambridge University Press, p.109

Schlegel D. J., Finkbeiner D. P., Davis M., 1998, ApJ, 500, 525

Southworth J., Smalley B., Maxted P. F. L., Claret A., Etzel P. B., 2005, MNRAS, 363, 529

van Leeuwen F., 2007, A&A, 474, 653